Iraqi Journal of Veterinary Sciences, Vol. 37, Supplement III, 2023 (111-119)
Proceedings of the 7th (2nd International) Scientific Conference, College of Veterinary Medicine, University of Al-Qadisiyah

Iraqi Journal of Veterinary Sciences

www.vetmedmosul.com

Modulation of chitosan nanoparticles properties for sheep pox mucosal vaccine delivery with cytotoxicity and release Studies-in vitro

M.R. Al-Zubaidi[1], H.T. Thwiny[1] and M.N. Al-Biati[2]

[1]Department of Microbiology, College of Veterinary Medicine, University of Basrah, Basrah, [2]Department of Chemistry, College of Education for Pure Sciences, University of Kerbala, Kerbala, Iraq

Article information

Article history:
Received 19 December, 2022
Accepted 10 November, 2023
Available online 09 December, 2023

Keywords:
Sheep pox
Chitosan
Nanoparticle
Toxicity

Correspondence:
M.R. Al-Zubaidi
mazin.r@uokerbala.edu.iq

Abstract

Sheep pox virus (SPPV) is a type of *Capripoxviruses* causing severe sheep infection that threatens the livestock industry worldwide. Currently, live SPPV vaccines are administered by parenteral route. To support facile mass vaccination while further enhancing mucosal immune responses, we developed chitosan nanoparticles (CS-NPs) for the mucosal delivery of a live SPPV vaccine. We investigated the effect of main factors on the physicochemical characteristics of the prepared NP properties. In the first set of experiments, we varied the formulation factors: CS concentrations, TPP concentrations, and CS: TPP volume ratios. In the second set, we investigated the effect of different CS:SPPV ratios. All experiments used the ionic gelation method to reach the optimal formulation. Based on the Dynamic Light Scattering (DLS) results, optimal blank CS-NPs formation had minimal, 85±30nm, and CS-NPs containing the live virus vaccine (LSPV-CS-NPs) was 458±17nm with regular spherical morphology by transmission electron microscope (TEM). LSPV-CS-NPs exhibited higher encapsulation efficiency 81±5.3%. FT-IR scans conferred cross-linking of functional groups. At 37°C, the release profile was faster in phosphate buffer solution (PBS) of pH five than in the physiological solution of PBS at the same temperature. The cytotoxicity effect of LSPV-CS-NPs was low, and results showed a high viability rate for cell culture in the presence of the nanoparticles. Our findings indicated a significantly efficient methodology of LSPV encapsulated in chitosan nanoparticles. LSPV-CS-NPs formulation is a candidate vaccine with preferred properties for mucosal immunization. This study lays a foundation for the following trials to test vaccine validity.

DOI: 10.33899/ijvs.2023.137403.2682,

Introduction

Sheep pox virus (SPPV) is a type of *Capripoxviruses*, which appears under an electron microscope as double-stranded DNA, enveloped virus sized over 350 nm with an oval or brick shape (1). SPPV is widespread in Iraqi farms, such as other viral diseases (2-5). SPPV causes drastic infections in sheep with high morbidity and mortality rates that threaten the livestock industry worldwide, and abortion is occasionally seen in ewes (6). Currently, animals are immunized against sheeppox by periodically injecting attenuated live or inactivated strains of SPPV via the parenteral route. This type of administration for the vaccine has several obstacles, resulting in the emergence of disease in sheep from one time to another (7). However, it seems there are defects related to low vaccination coverage or flaws in the validity of the vaccine, which always needs cold conditions for stores. Thus, an outbreak is highly anticipated at any time. Therefore, vaccines are required to overcome the determined limitations and facilities for mass vaccination. Mucosal immunization as a feasible strategy attracts the interest of researchers, depending on the truth (Know your enemy to find your friend) that most respiratory pathogens entrance into the mucosal site first, and pathogens can leak

into circulation across the mucosal barriers; it is being more reasonable that leads to induction double layers of integration immune responses at the mucosal surface paired to the systemic compartments. Mucosal immunization has been affirmed to potentiate antigen-systemic immune response equivalent to that caused by injection (8). In recent years, with the support of modern biotechnology, several research groups have demonstrated that nanocarriers are a promising strategy in biomedical applications due to their ability to efficient vaccine delivery into several target cells, which have advantages over subunit soluble antigens, inactivated viruses, or even live vaccines (9). Empirically, particles with uniform shape, ranging in nanoscale size between 1-1000 nm, and having neutral or positive surface charge are considered adequate to carry antigens and efficiently deliver them into target cells (10). However, among various nanoparticle approaches in biomedical applications, the vaccine delivery challenges have remained an emerging approach (11). Chitosan and its derivatives with numerous unique nanoparticle (NP)-based platforms appear as one of the most frequently mentioned polymers in the life sciences research studies, handling an extensive range for delivery nanosystems (12). In 2021 and 2022, market analysis reports. Market research future both have been valued size the global chitosan market at around USD 6.8-8.7 billion, and they are expected to expand into 24.7% to 25.9% by 2027 and 2030 respectively. The importance of these polymers is evident when observing the number of articles and patents that appear every year and the growing market perspective. The chitin is an amino polysaccharide naturally present in exoskeleton crustaceans, a linear homopolymer composed of *N*-acetyl-d-glucosamine bonded via the β(1→4) linkage (13). The uses of chitin are limited due to its low solubility in aqueous systems. This behavior of chitin is attributed to the presence of acetyl groups that can be removed by partial deacetylation in an alkaline environment to produce new compounds known by the generic name of chitosan (14,15). Chemically, the chitosan structure consists of a β- (1,4)-linked-D-glucosamine residue with the amine groups randomly acetylated (16). Chitosan has more solubility in acidic media under pKa value 6.5 (17) when around half of all amino groups are protonated, resulting in a polycationic biopolymer in water solution (18,19). This deacetylation procedure shows a high diversity of chitosan structures primarily depending on the deacetylation degree and pattern (20,21). Chitosan with 30-90% deacetylation degree can be obtained, but above 55 percent is ratio-dependent in most delivery system trials (our observation). The degree of deacetylation and molecular weight affect many of its chemical and physical properties that must be considered when choosing the best polymer for efficient vaccine delivery (22-24). This polysaccharide has been reported to have good biological features for nano-level applications compared to other materials, attributed to its good biocompatibility, biodegradability, adsorption, poor toxicity, and mucoadhesion (25). Moreover, its cationic character favors virus encapsulation and cellular internalization. Those properties transform this particular polymer into a promising material to develop Sheep pox vaccine delivery in nanosystems as a novel vaccination modality. In veterinary medicine, several studies in poultry and livestock industries have recently described chitosan carriers as suitable for Nano-system to deliver viral components (26-29).

The current study thoroughly explored the conditions for ionotropic chitosan gelation as a potential natural polymer for the suitable encapsulation and release profile to deliver a sheep pox virus vaccine against sheep pox infection in lambs. Other supportive studies to evaluate cytotoxicity value, stability, distribution, particle size, and surface charge of sheep pox virus-chitosan nanoparticles to ensure cellular internalization and replication *in vitro*. To achieve this and to design the optimal formulation of the sheep pox Nano-vaccine, we optimized CS-NPs by varying the TPP concentrations and chitosan at different volume ratios, then adjusted the volume ratio of chitosan into live SPPV suspension to obtain the optimal formulation of LSPV-CS-NPs.

Materials and methods

Reference SPPV

Lyophilized SPPV attenuated strain with a titer of 10^6 TCID50/ ml was kindly obtained from AL-Kindi Veterinary Drug and Vaccine Company of the Iraqi Industry Ministry, Baghdad, Iraq. This strain was reconstituted in 100 ml phosphate-buffered saline PBS. The live virus suspension was used in nanoparticle vaccine preparations and cellular investigations.

Preparation of Chitosan Solutions and TPP Solutions

Chitosan Powder (molecular weight lower than 150 kDa with DD 80-85% from sigma) was slowly dissolved in an aqueous solution slightly acidified with 1% acetic acid. This solution was continuously stirred at ambient temperature to obtain a perfectly homogeneous and transparent solution. Once dissolved, the chitosan solution was filtered through a 0.22 mm filter. The Final chitosan produced as a stock solution of 0.4 % w/v was diluted with deionized water to make chitosan solutions of different concentrations at 0.5 mg/ml, 1.0 mg/ml, and 1.5 mg/ ml. TPP (from sigma) was dissolved in deionized water at concentrations of 0.5 mg/ml, 1.0 mg/ml, and 2 mg/ml. The pH value of all experiment solutions was adjusted to six by adding NaOH. This study conducted control experiments, as SPPV chitosan nanoparticles were prepared in different concentrations of chitosan: SPPV:TPP ratios to identify optimal formulation 'recipe' producing nanoparticles of desirable characteristics for further studies.

Development of SPPV-chitosan-nanoparticles formulation

The chitosan-SPPV nanoparticles were prepared using an ionic cross-linking method earlier described by Calvo *et al.* (30) with slight modification. One volume of SPPV solution was added dropwise into two volumes of chitosan solution under magnetic stirring. Later, one volume of TPP solution was added drop by drop to the above solution. Subsequently, the chitosan-SPPV nanoparticles were formed spontaneously under agitation at room temperature. Ten minutes later, the chitosan-SPPV nanoparticles were separated by centrifugation at 10,000 rpm for 30 min at 4 °C. Then the supernatant was discarded, and the deposit was washed twice with distilled water. After centrifugation, chitosan-SPPV nanoparticles were re-dispersed in distilled water, and the product was lyophilized for 24 h using a vacuum freeze-drying machine (BOC Edwards Co. Ltd, UK) and stored at -20 C until required for further analysis. These nanoparticles were named LSPV-Cs-NPs. Unloaded CS-NPs were prepared as a control.

Optimization conditions of the SPPV-C-NPs preparation

Several factors affected the characteristics of the LSPV-CS-NPs, including the concentrations of chitosan, TPP solutions, and SPPV/CS ratio (v/v); the pH value at 6 was fixed for reactions. Single-factor experiments on the effects of the preparation condition of LSPV-C-NPs were conducted. Based on the results obtained in single-factor experiments, the key factors were SPPV/CS ratio (v/v), CS concentration, and TPP concentration. The agitating velocity was fixed at 700 rpm for 30 min at ambient temperature. Three factors and three levels were designed. All the key factors were examined, and size, morphology, PDI, and zeta potential with encapsulation efficiency were used as indicators (Table 1).

Table 1: Experimental design for preparation Cs-NPs and LSPV-Cs-NPs

Parameter	Lot#	CS (mg/ml)	TPP (mg/ml)	CS/TPP (ml/ml)	SPPV/CS (ml/ml)
CS concentration	F 1	0.5	0.5	2:1	1:1
	F 2	1.0	0.5	2:1	1:1
	F 3	1.5	0.5	2:1	1:1
TPP concentration	F 4	1.0	0.5	2:1	1:1
	F 5	1.0	2.0	2:1	1:1
CS: TPP volume ratio	F 6	1.0	0.5	1:1	1:1
	F 7	1.0	0.5	2:1	1:1
	F 8	1.0	0.5	2:1	1:1
LSPV:CS volume ratio	F 9	1.0	0.5	2:1	1:2
	F10	1.0	0.5	2:1	1:3

Nanoparticle's size and surface charge characterization

The particle sizes, zeta potentials, and polydispersity index (PDI) were measured using a Zeta Sizer 2000 (Malvern Instruments, United Kingdom, UK). In brief, 1 mg of the dried LSPV-C-NPs formulations was suspended in 1 mL of deionized water. Next, 50 µL of the stock was diluted in 1 mL of deionized water. Nanosuspensions were transferred to a cuvette and sonicated before determinations, placed in the Zetasizer, and equilibrated for 2 min. When the instrument was run, the laser emitted light with a wavelength of 633 nm; the scattered light was detected at a scattering angle of 90 degrees and a temperature of 25 °C.

Transmission electron microscopy (TEM) analysis

The morphology of LSPV-Cs-NPs was observed by TEM (Hitachi Ltd, Japan) (31). Briefly, the colloidal nanosuspension of each nanoparticles sample was sonicated for 2 min for better dispersion and to prevent particle agglomeration on the copper grid. The prepared sample was pipetted onto a carbon-coated copper grid. One drop of colloidal suspension was spread after being air-dried at room temperature for 24 hours; the sample was installed on the instrument and observed for imaging using a transmission electron microscope.

Fourier transform infrared spectroscopy (FTIR)

Lyophilized CS-NPs or LSPV-Cs-NPs were mixed with KBr powder and pressed into flakes. FTIR values of cross-linking were recorded by (FT-IR-instrument Bruker spectrophotometer, USA). All samples were measured in the frequency range of 400-4000 cm^{-1} for changes in the intensity of the sample peaks.

Evaluation of LSPV encapsulation percentage

The encapsulation efficiency of LSPV-CS-NPs was determined by separating the nanoparticles from the aqueous medium containing the free virus using centrifugation at 30,000 rpm for 30 min at 4 C. The amount of free LSPV in the supernatant was measured spectrophotometrically using a standard Bradford assay using Coomassie Brilliant Blue G-250 at 595 nm. All the measurements were performed in triplicate. The encapsulation efficiency (EE) of the

nanoparticles was calculated as EE (%) = (W0 -W1)/ W0 X100%. W0 is the total amount of LSPV added, and W1 is the amount of free LSPV.

In vitro evaluation of the safety of LSPV-CS-NPs

The cytotoxic effect of nanoparticles samples was estimated by a standard 3-(4,5-dimethyl-2-thiazolyl)- 2,5-diphenyl-2H-tetrazolium bromide (MTT, Sigma) test as was described earlier (32). Dehydrogenases reduce MTT in living cells to obtain a purple-colored product (formazan), which can be used for cytotoxicity assay by assessing optical density. Vero cells (ATCC® reference CCL-81™) were cultured in Minimal Essential Medium (MEM) supplemented with 10% fetal calf serum FCS. Cell culture was incubated in a humidified 37 °C with 5% CO_2. Cells were collected in 25 cm^2 culture flasks after dissociating adherent cells from surfaces by trypsinization in 2-3 min. Freshly 100 µl of cell suspension mixed gently with an equal volume of Trypan blue and viable cells were counted by hemocytometer technique. For the assay, $1x10^5$ Vero cells/ml were transferred to 96-well plates at 100 µl per well and cultured at 37 C for 24 h. After 100 µl of LSPV-Cs-NPs (diluted in MEM at 1.5 µg /ml) were added into the wells, the same volume of unloaded CS-NPs and original SPPV fluid were used as comparison controls. The plate was incubated at 37C for 24 h. ten µl MTT-containing medium (0.5 mg/mL) was added to the wells. Following three h incubation at 37 °C, the MTT-containing medium was carefully aspirated to avoid disturbing formed formazan crystals, and 100µL of solubilization solution DMSO was added to each well. Plates were incubated at room temperature for 30 min, and optical densities were determined at 570 nm using a microplate reader (DNM-9602, Beijing Prolong New Technology Co., LTD., Nanjing, China). Cell viability was expressed as a percentage of the untreated control cells. The survival rate of the cells was calculated as Survival rate % = [(At-Ab) / (Ac-Ab)] x100. Where at represents the test wells (containing LSPV- C-NPs, empty CS-NPs or SPPV); Ac represents the control wells (containing untreated control cells); and Ab represents the blank wells (containing the cell-free medium). All wells were subjected to the MTT assay procedure.

***In vitro* release profile of LSPV in different conditions**

Determination of release LSPV from LSPV-CS-NPs was performed by weighing 0.1 g of dried LSPV-C-NPs mixed with 2 ml of PBS (buffered in pH 7.4 and pH 5.0). The sealed tubes were placed in a water bath maintaining a temperature of 37±1 ◦C and stirred under agitation (50 rpm). Samples were withdrawn at regular intervals and centrifuged at 30,000 rpm for 10 min at 4 °C. LSPV concentration in the supernatant was measured by Bradford assay at 595 nm. After the sample was taken each time, the same volume of fresh PBS solution was added. The experiments were analyzed in triplicate. An LSPV release curve of LSPV-CS-NPs was plotted against the release time at the X-axis and the accumulative release amount at the Y-axis.

Statistical analysis

GraphPad Prism version 8 was used to perform the statistical analysis. Also, two-way analysis of variance (ANOVA) and Tukey's multiple comparison tests were used to analyze the obtained data. Data were shown as mean and standard deviation (33).

Results

Optimization formula of nanoparticles

Depending on the optimal values of the selected variables, the best conditions were in F2 expressed for CS-NPs, and F9 represented optimal values that can be formulated for LSPV-CS-NPs. Physiochemical characterizations were average at 85±30 nm with PDI 0.3±0.05 and surface charge at 31±4 mV for F2. At the same time, F9 was 458±17nm, PDI 0.2±0.09 and surface charge 43±6 mV with highest encapsulation efficiency of 81±5.3%. As determined by DLS, particle size was significantly correlated to the volume ratio of SPPV: CS, where nanoparticles size increased with higher or lower volume content of CS in the experiment. However, CS and TPP concentrations were significant factors in the formulation of CS-NPs or LSPV-CS-NPs in all experiments, as the size of nanoparticles was linearly increased with increasing TPP (Table 2).

Table 2: Optimization CS-NPs and LSPV-CS-NPs

Lot#	mean±S.D (n=3)		
	Hydrodynamic diameter (nm)	Zeta potential (mV)	PDI Index
F 1	114±24	27±3	0.3±0.02
F 2	85±30	31±4	0.3±0.05
F 3	334±31	12±2	0.5±0.06
F 4	117±16	16±2	0.3±0.03
F 5	392±70	20±1	0.4±0.05
F 6	286±12	16±6	0.5±0.07
F 7	236±27	15±5	0.5±0.07
F 8	533±62	52 ±3	0.3±0.12
F 9	458±17	43±6	0.2±0.09
F10	627±62	38±1	0.4±0.05

Microscopic study using TEM

The TEM analysis of nanoparticles exhibited regularly formed and well distributed in acetic acid solution (pH 6.0) was used in this study. The morphology of viral particles encapsulated with chitosan nanoparticles appeared dark and smooth spherical shaped with moderately uniform particle size and even distribution as depicted by TEM (Figure 1) at magnification 25000. Proteins from membrane-attached filaments project from the external membrane in distinctive arrangement for SPPV were observed.

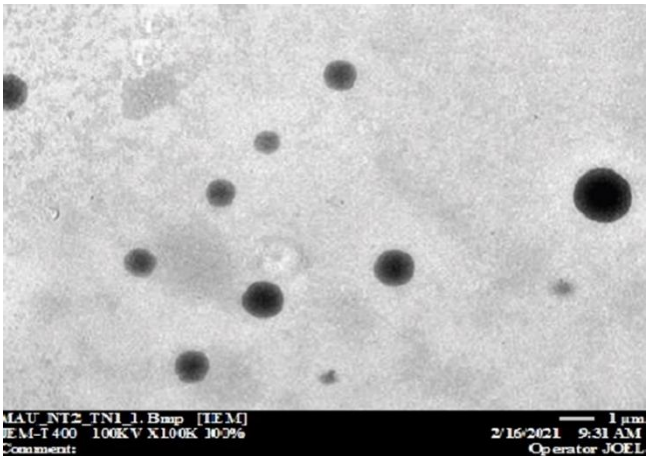

Figure 1: TEM Image for LSPV-CS-NPs.

FT-IR Analysis

Figure 2 showed weak broadband at 3422 cm^{-1} attributed to the bond O-H alcoholic and H-bonded, also showed a two peak at ~3700 cm^{-1} attributed to the NH_2 stretching bonds, and a stretching band at the 2937cm^{-1} back to N-Methyl bond, also shows a solid stretching band at 1648 cm^{-1} back to the N-H bending bond, and a peak at 1078, 1025 cm^{-1} of the C-N amine, C-O alcoholic bonds. Figure 2 B showed fragile broadband at 3009 cm^{-1} attributed to the O-H carboxylic bond and H-bond and showed a stretching band at 3004 cm^{-1} and 2970 cm^{-1} attributed to the symmetric and asymmetric C-H bonds, also showed a peak at 3463 cm^{-1} attributed to the N-H stretching bond, and stretching bands at 2527 and 2651cm^{-1} back to N-Methyl bonds, also a solid stretching band at 1738 cm^{-1} back to the C=O bond, also shows a band at 1566,1402 cm^{-1} back to the N-H, O-H carboxylic bending bonds, and a peak at 1231, 1070 cm^{-1} of the C-N amine, C-O carboxylic bonds.

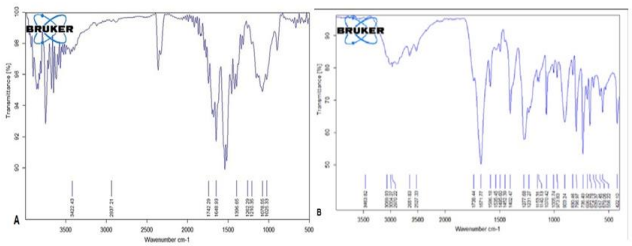

Figure 2: FT-IR spectroscopy of (A) CS-NPs and (B) LSPV-CS-NPs

Effects of LSPV-CS-NPs induced cytotoxicity on Vero cells

The survival rate of Vero cells in wells containing LSPV-CS-NPs was 93.28±2.67%, and no significant change in cell morphology was observed compared with the control cells (Figure 3).

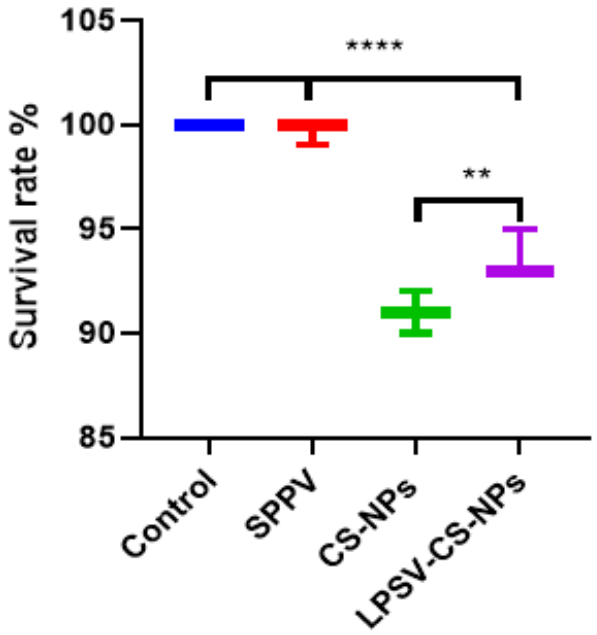

Figure 3: Cell survival rate percentages were assessed by MTT assay. The results represent the means of at least three independent experiments. The cell viability was observed after MTT treatment in the indicated Vero cells after 24 h underexposure. Value in the graph represents the means standard deviation of three independent. ****P<0.0001 vs. control and SPPV; **P<0.001 vs. CS-NPs.

Effect of pH degree on release LSPV of LSPV-CS-NPs

The cumulative release rates of LSPV particles from nanoparticle formulation (Figure 4). The result obtained in vitro was determined according to simulated artificial nasal cavity acidity compared to physiological PBS. It can be seen from the effects that the initial release of the LSPV in acidic conditions at first 12 h was 44.15 ± 2.62 %, while in physiological PBS, it was 27.23± 1.12%. The LSPV-CS -NPs continued to release and escalate throughout the experiment in both condition and was faster in pH 5.0 after 24 h. However, the subsequent release was relatively steady for both states involved in this study. At the end of the trial period, the cumulative release at acidic pH reached 86.93± 2.27%; nevertheless, it was still higher compared to parallel experiments at pH 7.4, it was no more than 61.78 ± 1.42%.

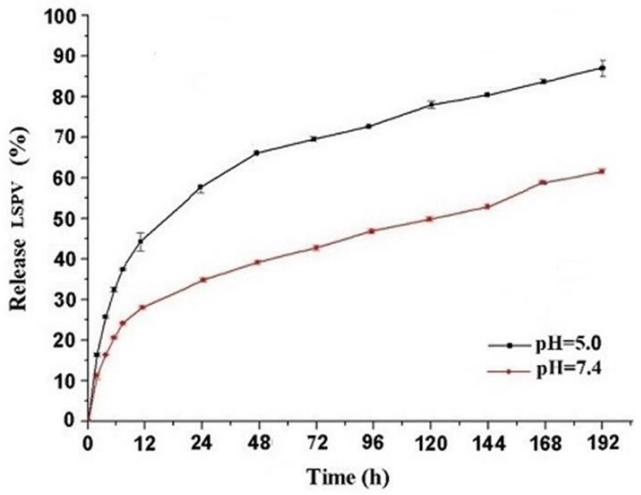

Figure 4: In vitro release profiles of LSPV from LSPV-CS-NPs in PBS (pH 7.4 & 5.0). The experiment was repeated three times, and each was measured in triplicate. Data were presented as mean values ±SD.

Discussion

In veterinary medicine, immunization is the most effective way to improve livestock productivity. Nevertheless, SPPV causes a severe disease seen frequently in ovine flocks despite a preventive vaccine being in use. Therefore, there is an urgent need for new or developed vaccines to overcome the potential limitations. Regardless of the distinctive physicochemical properties of chitosan, it is an ideal polymer for carrying vaccines in the Nano-system and accessible into mucosal sites. Thus, this study was established as we worked to optimize the conditions to achieve minimum particle size with maximum encapsulation efficiency. Introducing a positive charge on the chitosan nanoparticle surface induces a favorable interaction with the negatively charged viral particles and the plasma membrane of targeted cells or mucus. This study used the ionic cross-linking method to prepare LSPV encapsulated in chitosan nanoparticles because SPPV is sensitive to organic solvents and temperature. The benefits of using whole live attenuated SPPV strain are multivalent, and it is expected to include more epitopes than single-antigen subunit vaccines; in addition, it maintains the ability to replicate, thus producing a vaccine with a high reactogenicity.

Experiments were conducted at specified optimal conditions to validate the model. The observed values confirmed complete agreement that the model was statistically significant. Therefore, this model has adequate precision for predicting optimum conditions in minimizing the particle size and maximizing the encapsulation efficiency. The size of chitosan nanoparticles obtained in small nm and charged positively enhances efficient entrapment for viral particles. Encapsulation is adopted in vaccine delivery systems to prevent it from leaching out before reaching the targeted site. These observations are consistent with the findings of Zhao *et al.* (34) and Akalya (35); they have demonstrated that it might attain the ability to attach to the target cells and increase the probability of cellular uptake. The LSPV encapsulation showed lower efficiencies for F8 and F10 compared to an increase in F9. EE may be affected by various factors; this result can be explained by chitosan polymer concentration proportionated to the density of LSPV and TPP. Moreover, the intermolecular interactions occur in the presence of oppositely charged reaction components. Therefore, the zeta potential is the most critical factor in determining the efficiency of the encapsulation process. The stability of chitosan nanoparticles is directly related to surface charge and zeta potential between - 30 to +30 mV, indicating a condition toward instability (36). The F9 was freeze-dried for zeta potential analysis. The colloidal suspension with a zeta potential of 40 to 60 mV is considered a desirable range, while lower values tend to coagulate or flocculate (37). The optimum F2 and F9 exhibited excellent stability in suspension at room temperature and -70 °C for long-term storage (data not shown). The particle size is another essential quality indicator affecting encapsulation and internalization efficiency. Particles (microparticles/nanoparticles) were identified at 100-500 nm as the optimal size range for cellular uptake primarily via endocytosis; this size range also allows for M cells to transport NPs (38,39). The morphology of nanoparticles is an important parameter determining the uptake pathway, and a spherical shape with a smooth surface is preferable. There is a body of evidence affirming that Polymeric nanoparticles with the same surface chemistry and various morphology exhibit different transport paths (40,41).

Next, FTIR studies were conducted to determine the compatibility of the virus with other formulation excipients. FTIR spectroscopy helps identify the functional groups and bonds present in the formulation. When comparing the FT-IR diagrams for both CS-NPs and LSPV-CS-NPs, we found a difference between the two charts in terms of the shapes of the absorption peaks resulting from the compounds on the one hand, and between the values of absorption frequencies for the functional groups present in each combination on the other hand. We observed that the presence of shifting of peaks caused the interaction of the virus with chitosan nanoparticles. This demonstrates the presence of interference and interdependence between the NPs Chitosan and the added virus, resulting in the formation of the LSPV-CS-NPs composite (32).

Cellular cytotoxicity is a critical issue to be analyzed when choosing the best delivery system to ensure its suitability for cellular uptake in vitro and in vivo assays. Our observations on the viability of Vero cells indicate good biocompatibility and moderate toxicity of LSPV-CS-NPs, with significant differences compared to the impacts of such

factors conducted in the assay. Chitosan nanoparticles coated LSPV less toxic on Vero cells than unloaded chitosan nanoparticles, and this related to the hypothesis of Wani and his colleagues (42) that the NPs average size, as well as the cationic surface charge directly elevated the toxicity risk. Therefore, a lower particle average size should increase the unloaded CS-NPs cytotoxicity activity on Vero cells. Conversely, the LSPV presence of CS-NPs shows increasing biocompatibility toward healthy Vero cells. The crude SPPV is not affected in Vero cells, and recorded levels are proximal to control throughout the investigation, which may indicate less cellular uptake and the successful internalization of LSPV-CS-NPs; it may be related to the high positive *zeta* potential caused by conjugated chitosan nanoparticles as chitosan nanoparticles have more excellent mucoadhesion property that promotes the increase of permeation onto Vero cells, conducting for higher rate cellular uptake of viral particles (43,44). The existing body of toxicological literature suggests clearly that nanoparticles may have a greater risk of toxicity than larger particles (45). However, nanoparticles produced from chitosan have a molecular weight of less than 15 kDa, and a deacetylation degree between 70% and 85% is the lowest cytotoxicity effect (46). We have therefore concluded that the formulation produced herein is safe enough to be used in sheep.

The synthesis process of nanoparticles in this study is by ionic gelation between different charges of chitosan and the other materials in the dissolved state. In vitro nanoparticles release of LSPV was in media at moderate acidic pH and neutralized pH in 37ºC; thus, when the pH condition of the media is changed from a suitable level, the electrostatic of the LSPV-CS-NPs formulation could be changed, resulting in reducing of gel nanoparticles formation (47). This could be explained by the initial burst at the first twelve hours, as the weak interaction of some formulation components. Furthermore, core materials encapsulated in nanoparticles can be released during physicochemical degradation of the particle structure. Therefore, one explanation for these results is that chitosan polymers tend to swell in acidic environments due to the protonation of the chitosan amino group. Thus, encapsulated LSPV could quickly diffuse out of the nanoparticles into the dissolution media. On the other hand, the release of LSPV from CS-NPs was at a lower gradual rate in neutral conditions compared to acidic conditions. Two main interaction mechanisms can explain this difference. One is the insolubility of chitosan at neutral pH. The formulation of LSPV-CS-NPs might be sustained since chitosan solubility in neutral conditions is substantially lower than in acidic conditions (48). Another possibility is the deprotonation of chitosan molecules at neutral pH, which could stabilize the nanoparticle structure due to the lack of amino group protonation and the formation of more hydrogen bonds, resulting in prolonged LSPV release (49,50). Using chitosan to prepare LSPV-based based-nanoparticles vaccine appears to be a potential regulator of the intranasal release of bioactive materials. Therefore, F9 prepared using CS and TPP seemed to have prolonged releasing. As a result, this leads to a sustained LSPV release. However, further studies are required.

Conclusions

We concluded that the successful synthesis of nano-SPPV vaccine with characteristics to deliver it into mucosal sites was achieved using a novel approach. The present investigation confirmed that the chitosan polymer at the nanoscale could be applied as a suitable matrix to design controlled release formulations of the SPPV vaccine with expected properties and release characteristics. Due to their integrity and unique mucosal adhesion ability, vaccine delivery systems based on CS-NPs enable transmucosal delivery as vaccine delivery vectors. The optimized LSPV-CS-NPs have the advantage of overcoming the primary defects of conventional vaccines and the facility for the mass free-inject vaccination in sheep. This study opens the door to next-generation vaccine delivery systems intended for mucosal administration, at least in ovine. The process of nano-vaccine manufacturing was relatively uncomplicated and may be implemented on a commercial industry scale in conventional vaccine manufacturing units. From the in-vitro studies, the formulations were promising and should be considered for bioavailability studies in the field to assess in-vivo characteristics.

Acknowledgment

The researchers extend their thanks and gratitude to University of Kerbala and Basrah University for supporting this study.

Conflict of interest

The authors declare that they have no competing interests.

References

1. Tulman ER, Afonso CL, Lu Z, Zsak L, Sur JH, Sandybaev NT, Kerembekova UZ, Zaitsev VL, Kutish GF, Rock DL. The genomes of sheepox and goatpox viruses. J Virol. 2002;76:6054-6061. DOI: 10.1128/JVI.76.12.6054-6061.2002
2. Mansour KA, Hussain MH, Abid AJ, Kshash QH. Orf disease in local goat; Clinical and phylogenetic study in Al-Qadisiyah governorate, Iraq. Iraqi J Vet Sci. 2022;36:(1):117-121. DOI: 10.33899/ijvs.2021.129489.1651
3. Mansour KA, Hassan HN, Muthanna HH. Phylogenetic tree analysis study of bovine papillomaviruses type 1 based on L1 gene in Al-Qadisiyah, Iraq. Iraqi J Vet Sci. 2019;33(1):151-155. DOI: 10.33899/ijvs.2019.125535.1057
4. Abdul Aziz JM, Salih AH, Hawre KF. Molecular diagnosis and genetic relationship of foot and mouth disease virus serotype

Asia1/Basne/Sul/2015. Iraqi J Vet Sci. 2019;33(1):67-73. DOI: 10.33899/ijvs.2019.125519.1041
5. Muhammed SW, Hasso SA, Abdulla FA. Serological diagnosis of FMD in sheep in Basra by ELISA test. Iraqi J Vet Sci. 2013;27(2):79-84. DOI: 10.33899/ijvs.2013.82785
6. Mahmoud MA, Ghazy AA, Shaapan RM. Review of diagnostic procedures and control of some viral diseases causing abortion and infertility in small ruminants in Egypt. Iraqi J Vet Sci. 2021;35(3):513-521. DOI: 10.33899/ijvs.2020.127114.1461
7. Noah IA, Rasheed SA. Effect of pox vaccine on blood picture in adult ewes. Basrah J Vet Res. 2020;19(2):24-31. DOI: 10.23975/bjvetr.2020.174094
8. Lavelle EC, Ward RW. Mucosal vaccines-fortifying the frontiers. Nat Rev Immunol. 2022;22(4):236-250. DOI: 10.1038/s41577-021-00583-2
9. Gregory AE, Titball R, Williamson D. Vaccine delivery using nanoparticles. Front Cell Infect Microbiol. 2013;3:13. DOI: 10.3389/fcimb.2013.00013
10. Calderon-Nieva D, Goonewardene KB, Gomis S, Foldvari M. Veterinary vaccine nanotechnology: Pulmonary and nasal delivery in livestock animals. Drug Deliv Transl Res. 2017;7:558-570. DOI: 10.1007/s13346-017-0400-9
11. Baden LR, El Sahly HM, Essink B, Kotloff K, Frey S, Novak R, Diemert D, Spector SA, Rouphael N, Creech CB, McGettigan J. Efficacy and safety of the mRNA-1273 SARS-CoV-2 vaccine. N Engl J Med. 2021;384(5):403-16. DOI: 10.1056/NEJMoa2035389
12. Bellich B, D'Agostino I, Semeraro S, Gamini A, Cesàro A. The Good, the Bad and the Ugly of Chitosans. Mar Drugs. 2016;14:99. DOI: 10.3390/md14050099
13. Kadokawa JI. Dissolution, gelation, functionalization, and material preparation of chitin using ionic liquids. Pure Appl Chem. 2016;88:621- 629. DOI: 10.1515/pac-2016-0503
14. Al-Obaidi AA, Al-Sadi HI, Hashim SS, Markas NH. Preparation and evaluation of cross-linked chitosan-polyurethane mesh in tissue repair in sheep. Iraqi J Vet Sci. 2006;20(2):145-161. DOI: 10.33899/ijvs.2006.62493
15. Leiva A, Bonardd S, Pino M, Saldías C, Kortaberria G, Radić D. Improving the performance of chitosan in the synthesis and stabilization of gold nanoparticles. Eur Polym J. 2015;68:419-431. DOI: 10.1016/j.eurpolymj.2015.04.032
16. Sevda S, McClureb SJ. Potential applications of chitosan in veterinary medicine. Adv Drug Deliv Rev. 2004;56:1467-1480. DOI: 10.1016/j.addr.2004.02.007
17. Domard A. pH and cd measurements on a fully deacetylated chitosan: application to CuII—polymer interactions. Int J Biol Macromol. 1987;9(2):98-104. DOI: 10.1016/0141-8130(87)90033-X
18. Rinaudo M, Pavlov G, Desbrieres J. Influence of acetic acid concentration on the solubilization of chitosan. Polymer. 1999;40(25):7029-32. DOI: 10.1016/S0032-3861(99)00056-7
19. Panos I, Acosta N, Heras A. New drug delivery systems based on chitosan. Curr Drug Discov Technol. 2008;5:333-341. DOI: 10.2174/157016308786733528
20. Rinaudo M. Chitin and chitosan: Properties and applications. Prog Polym Sci. 2006;31:603-632. DOI: 10.1016/j.progpolymsci.2006.06.001
21. Aranaz I, Mengíbar M, Harris R, Paños I, Miralles B, Acosta N, Galed G, Heras A. Functional characterization of chitin and chitosan. Curr Chem Biol. 2009;3:203-230. DOI: 10.2174/187231309788166415
22. Kiang T, Wen J, Lim HW, Leong KW. The effect of the degree of chitosan deacetylation on the efficiency of gene transfection. Biomater. 2004;25(22):5293-301. DOI: 10.1016/j.biomaterials.2003.12.036
23. Alameh M, Lavertu M, Tran-Khanh N, Chang CY, Lesage F, Bail M, Darras V, Chevrier A, Buschmann MD. siRNA delivery with chitosan: Influence of chitosan molecular weight, degree of deacetylation, and amine to phosphate ratio on in vitro silencing efficiency, hemocompatibility, biodistribution, and in vivo efficacy. Biomacromol. 2018;19(1):112-131. DOI: 10.1021/acs.biomac.7b01297
24. Popescu R, Ghica MV, Dinu-Pîrvu CE, Anuța V, Lupuliasa D, Popa L. New opportunity to formulate intranasal vaccines and drug delivery systems based on chitosan. Int J Mol Sci. 2020;21(14):5016. DOI: 10.3390/ijms21145016
25. Aranaz I, Alcántara AR, Civera MC, Arias C, Elorza B, Heras Caballero A, Acosta N. Chitosan: An overview of its properties and applications. Polymers. 2021;13(19):3256. DOI: 10.3390/polym13193256
26. Elmasry DM, Fadel MA, Mohamed FH, Badawy AM, Elsamadony HH. Copper chitosan nanocomposite as antiviral and immune-modulating effect in broiler experimentally infected with chicken anemia virus. Iraqi J Vet Sci. 2022;36(4):999-1009. DOI: 10.33899/ijvs.2022.132826.2135
27. Unsunnidhal L, Wasito R, Setyawan EN, Kusumawati A. Potential of nanoparticles chitosan for delivery pcDNA3.1-tat. BIO Web Conf. 2021;41:07004. DOI: 10.1051/bioconf/20214107004
28. Zhao K, Sun B, Shi C, Sun Y, Jin Z, Hu G. Intranasal immunization with O-2′-Hydroxypropyl trimethyl ammonium chloride chitosan nanoparticles loaded with Newcastle disease virus DNA vaccine enhances mucosal immune response in chickens. J Nanobiotechnol. 2021;19:1-5. DOI: 10.1186/s12951-021-00983-5
29. Pan L, Zhang Z, Lv J, Zhou P, Hu W, Fang Y, Chen H, Liu X, Shao J, Zhao F, Ding Y, Lin T, Chang H, Zhang J, Zhang Y, Wang Y. Induction of mucosal immune responses and protection of cattle against direct-contact challenge by intranasal delivery with foot-and-mouth disease virus antigen mediated by nanoparticles. Int J Nanomed. 2014;9(1):5603-5618. DOI: 10.2147/IJN.S72318
30. Calvo P, Remuñán-López C, Vila-Jato JL, Alonso MJ. Novel hydrophilic chitosan-polyethylene oxide nanoparticles as protein carriers. J App Polym Sci. 1997;63(1):125-132. DOI: 10.1002/(sici)1097-4628(19970103)63:1<125::aid-app13>3.0.co;2-4
31. Hameed A, Aahmed J. The medical applications of transmission electron microscope: Subject review. Basrah J Vet Res. 2021;20(2):80-83. DOI: 10.23975/bvetr.2021.170500
32. Zaboon MH, Saleh AA, Al-Lami HS. Synthesis, characterization and cytotoxicity investigation of chitosan-amino acid derivatives nanoparticles in human breast cancer cell lines. J Mex Chem Soc. 2021;65(2):178-188. DOI: 10.29356/jmcs.v65i2.1265.
33. Mahmoud MA, Khafagi MH. Detection, identification, and differentiation of sheep pox virus and goat pox virus from clinical cases in Giza Governorate, Egypt. Vet World. 2016;9(12):1445-1449. DOI: 10.14202/vetworld.2016.1445-1449
34. Zhao K, Chen G, Shi XM, Gao TT, Li W, Zhao Y, Zhang FQ, Wu J, Cui X, Wang YF. Preparation and efficacy of a live Newcastle disease virus vaccine encapsulated in chitosan nanoparticles. PloS One. 2012;7(12):e53314. DOI: 10.1371/journal.pone.0053314
35. Akalya J, Srithar A, Thangavelu A, Parthiban M. Preparation and evaluation of chitosan encapsulated live Peste des petits ruminants (PPR) virus vaccine. Indian Vet J. 2017;94(10):27-9. [available at]
36. Pan C, Qian J, Zhao C, Yang H, Zhao X, Guo H. Study the relationship between crosslinking degree and properties of TPP crosslinked chitosan nanoparticles. Carbohydr Polym. 2020;241:116349. DOI: 10.1016/j.carbpol.2020.116349
37. Yu W, Xie H. A Review on nanofluids: Preparation, stability mechanisms, and applications. J Nanomater. 2012;2012:1-17. DOI: 10.1155/2012/435873
38. Kaksonen M, Roux A. Mechanisms of clathrin-mediated endocytosis, Nat Rev Mol Cell Biol. 2018;19:313-326. DOI: 10.1038/nrm.2017.132
39. de Almeida MS, Susnik E, Drasler B, Taladriz-Blanco P, Petri-Fink A, Rothen-Rutishauser B. Understanding nanoparticle endocytosis to improve targeting strategies in nanomedicine. Chem Soc Rev. 2021;50:5397-5434. DOI: 10.1039/D0CS01127D
40. Salatin S, Khosroushahi AY. Overviews on the cellular uptake mechanism of polysaccharide colloidal nanoparticles. J Cell Mol Med. 2017;21(9):1668-86. DOI: 10.1111/jcmm.13110
41. Ridolfo R, Tavakoli S, Junnuthula V, Williams DS, Urtti A, van Hest JC. They are exploring the Impact of morphology on the properties of biodegradable nanoparticles and their diffusion in complex biological medium. Biomacromol. 2021;22(1):126-133. DOI: 10.1021/acs.biomac.0c00726

42. Wani MY, Hashim MA, Nabi F, Malik MA. Nanotoxicity: Dimensional and morphological concerns. Adv Phys Chem. 2011;2011:15. DOI: 10.1155/2011/450912
43. Caramella C, Ferrari F, Bonferoni MC, Rossi S, Sandri GJ. Chitosan and its derivatives as drug penetration enhancers. Drug Deliv Sci Technol. 2010;20:5-13. DOI: 10.1016/S1773-2247(10)50001-7
44. Chen MC, Mi FL, Liao ZX, Hsiao CW, Sonaje K, Chung MF, Hsu LW, Sung HW. Recent advances in chitosan-based nanoparticles for oral delivery of macromolecules. Adv Drug Deliv Rev. 2013;65:865-879. DOI: 10.1016/j.addr.2012.10.010
45. Ramakrishna D, Rao P. Nanoparticles: Is toxicity a concern?. Electron J Int Fed Clin Chem Lab Med. 2011;22(4):92-101. [available at]
46. Herdiana Y, Wathoni N, Shamsuddin S, Muchtaridi M. Drug release study of the chitosan-based nanoparticles. Heliyon. 2021;8(1):e08674. DOI: 10.1016/j.heliyon.2021.e08674
47. Huang GQ, Xiao JX, Jia L, Yang J. Complex coacervation of O-carboxymethylated chitosan and gum Arabic. Int J Polym Mater Polym Biomater. 2015;64:198-204. DOI: 10.1080/00914037.2014.936591
48. Kim ES, Baek Y, Yoo HJ, Lee JS, Lee HG. Chitosan-tripolyphosphate nanoparticles prepared by ionic gelation improve the antioxidant activities of astaxanthin in the in vitro and in vivo model. Antioxidants. 2022;11(3):479. DOI: 10.3390/antiox11030479
49. Anitha A, Deepagan V, Rani VD, Menon D, Nair S, Jayakumar R. Preparation, characterization, in vitro drug release and biological studies of curcumin loaded dextran sulphate-chitosan nanoparticles. Carbohydr Polym. 2011;84:1158-1164. DOI: 10.1016/J.CARBPOL.2011.01.005
50. Chang W, Liu F, Sharif HR, Huang Z, Goff HD, Zhong F. Preparation of chitosan films by neutralization for improving their preservation effects on chilled meat. Food Hydrocoll. 2019;90:50-61. DOI: 10.1016/J.FOODHYD.2018.09.026

تغير وملائمة خصائص جزيئات النانو لشيتوزان لتوصيل لقاح جدري الأغنام الى الأنسجة المخاطية مع دراسة السمية والتحرر في المختبر

مازن رزاق كاظم الزبيدي[١]، حازم طالب ثويني[١] و محمد ناظم بهجت البياتي[٢]

[١]فرع الأحياء المجهرية، كلية الطب البيطري، جامعة البصرة، البصرة، [٢]قسم الكيمياء، كلية التربية للعلوم الصرفة، جامعة كربلاء، كربلاء، العراق

الخلاصة

يسبب فيروس جدري الأغنام إصابات خطيرة في قطعان الأغنام. ويتصف المرض بمعدلات إمراضية ووفيات عالية، عادة ما تهدد تجارة وصناعة اللحوم حول العالم. في الوقت الحاضر تعطى اللقاحات الحية المضعفة ضد جدري الأغنام عن طريق الحقن. في هذه الدراسة طورنا لقاح يعتمد على جزيئات الشيتوزان النانوية لإيصال اللقاح الى الأغشية المخاطية، وذلك لزيادة تحفير المناعة المخاطية ويساهم بتسهيل عملية التلقيح لقطعان الأغنام. لقد تم فحص تأثير العوامل الرئيسية على تكوين الجزيئات النانوية حيث أجريت المجموعة الأولى من التجارب من خلال تغير تراكيز ثلاثي متعدد الفوسفيت مع تراكيز الشيتوزان وأنتجت أفضل مكون لجزيئات النانو لشيتوزان - ثلاثي متعدد الفوسفيت وفي المجوعة الثانية من التجارب تم دراسة وفحص تأثير النسب الحجمية بين معلق الفيروس والشيتوزان. كل التجارب أجريت بطريقة التأين الهلامي للحصول على التركيب الأمثل. وبالاعتماد على نتائج مسح توزيع الإشعاع كان أفضل لجزيئات النانو لشيتوزان-ثلاثي متعدد الفوسفيت هو ٨٥±٣٠ نانوميتر مع ٤٥٨±١٧ نانوميتر لجزيئة النانو المكون من فيروس وشيتوزان. وأظهرت نتائج فحص المجهر الإلكتروني شكل كروي واضح ومنتظم. وكانت كفاءة التغليف تصل الى ٨١±٥,٣%. وقد أكد ذلك فحص الارتباط للمجاميع الفعالة بين الفيروس والشيتوزان على المستوى النانوي. تمت دراسة تحرر الفيروس في الوسط الحامضي حيث كان التحرر أسرع مما في الوسط المتعادل، بينما أظهرت دراسات السمية تأثير طفيف مع معدلات حيوية عالية لخلايا الزرع. بشكل عام دلت نتائجنا على كفاءة التغليف للشيتوزان النانوي وان تركيبة الفيروس شيتوزان نانوجزيئي هو لقاح مرشح يمتلك خصائص ملائمة للتمنيع المخاطي. أن هذه الدراسة وضعت أساسا لتجارب قادمة تختبر اللقاح في الحقل.